Acta Crystallographica Section B
Structural Science
ISSN 0108-7681

Polymorphism in the nitrate salt of the $[Mn(acetylacetonate)_2(H_2O)_2]^+$ ion

A. R. Biju and M. V. Rajasekharan*

School of Chemstry, University of Hyderabad, Hyderabad, Andhrapradesh 500046, India

Correspondence e-mail: mvrsc@uohyd.ernet.in

Received 10 August 2009
Accepted 17 March 2010

The crystallization of $[Mn(acac)_2(H_2O)_2]^+$ from solutions containing excess nitrate leads to the formation of four polymorphs. All polymorphs contain two different types of complex ions, one containing essentially coplanar acac ligands and the other in which the two acac ligands together assume a chair conformation. Molecular modelling using DFT (density-functional theory) calculations shows that the coplanar conformation is the electronically stable one. The hydrogen bonding between the *trans*-water molecules and the nitrate ion produces a one-dimensional chain of 12-membered rings, which are further organized into a two-dimensional network *via* a lattice water molecule. Lattice-energy calculations have been carried out to compare the stabilities of the four polymorphs.

1. Introduction

The crystal structure determination of $[Mn(acac)_2(H_2O)_2]ClO_4 \cdot 2H_2O$, bis(acetylacetonato)diaquamanganese(II) perchlorate dihydrate (Swarnabala *et al.*, 1994), provided a rare comparison of the coordination polyhedron of a Jahn–Teller-active d^4 complex with the analogous, inactive d^5 complex, *viz.* $[Mn(acac)_2(H_2O)_2]$, where acacH = acetylacetone. With a view to developing this comparison into a college chemistry experiment, we attempted the preparation of the d^4 complex cation as a more student-friendly nitrate salt. Quite unexpectedly, this resulted in four polymorphs of the monohydrate of the nitrate. The structures and lattice-energy calculations of these polymorphs are reported in this paper. Since polymorphism as well as the high Z' value (the number of crystallographically different formula units per asymmetric unit) observed are thought to be related to hydrogen bonding, a tetrafluoroborate salt, for which no polymorphs were obtained under the conditions used, was also prepared and characterized for comparison. The phenomenon of polymorphism (Bernstein, 2002) has generated much interest in recent times, in part due to its importance – biological as well as commercial – in pharmaceutical science. However, since making a polymorph at will is often difficult, a systematic study, whenever the phenomenon is observed, is important.

2. Experimental

2.1. General methods and materials

All chemicals were purchased from Ranbaxy chemicals and used without further purification. IR spectra were obtained with a Shimadzu FT-IR 8000 spectrometer. Elemental analysis was obtained using a Flash EA 1112 Series CHNS analyzer.

© 2010 International Union of Crystallography
Printed in Singapore – all rights reserved

doi:10.1107/S0108768110009961

Table 1

Crystallographic data for $[Mn(acac)_2(OH_2)_2]NO_3 \cdot H_2O$ [(1), (2), (3) and (4)] and $[Mn(acac)_2(OH_2)_2]$ BF_4 (5).

Experiments were carried out with Mo *Kα* radiation using a CCD area-detector diffractometer. Empirical absorption (using intensity measurements) using *SADABS*.

	(1)	(2)	(3)	(4)	(5)
Crystal data					
Chemical formula	$C_{10}H_{18}MnO_6 \cdot NO_3 \cdot H_2O$	$C_{10}H_{18}MnO_6 \cdot NO_3 \cdot H_2O$	$C_{10}H_{18}MnO_6 \cdot NO_3 \cdot H_2O$	$C_{10}H_{18}MnO_6 \cdot NO_3 \cdot H_2O$	$C_{10}H_{22}BF_4MnO_8$
M_r	369.21	369.21	369.21	369.21	412.03
Crystal system, space group	Triclinic, $P\overline{1}$	Triclinic, $P\overline{1}$	Triclinic, $P\overline{1}$	Monoclinic, $P2_1/c$	Monoclinic, $C2/m$
Temperature (K)	298	298	298	100	100
a, b, c (Å)	7.7085 (7), 7.7158 (7), 15.9918 (14)	7.902 (4), 13.238 (7), 15.966 (8)	7.901 (4), 13.298 (7), 16.832 (8)	7.8378 (5), 12.9697 (8), 31.268 (2)	7.5897 (6), 11.8987 (10), 10.2350 (8)
α, β, γ (°)	97.8890 (10), 91.533 (2), 118.3800 (10)	86.226 (8), 80.642 (8), 89.990 (8)	109.655 (7), 94.745 (8), 90.033 (8)	90.00, 94.6900 (10), 90.00	90.00, 110.5490 (10), 90.00
V (Å^3)	824.28 (13)	1644.2 (14)	1659.0 (14)	3167.9 (3)	865.49 (12)
Z	2	4	4	8	2
μ (mm^{-1})	0.85	0.85	0.84	0.88	0.84
Crystal size (mm)	0.24 × 0.20 × 0.20	0.24 × 0.18 × 0.16	0.24 × 0.22 × 0.18	0.38 × 0.36 × 0.28	0.32 × 0.23 × 0.20
Data collection					
T_{min}, T_{max}	0.823, 0.849	0.822, 0.876	0.824, 0.863	0.731, 0.790	0.776, 0.851
No. of measured, independent and observed [$I > 2\sigma(I)$] reflections	8507, 3194, 2677	17 286, 6520, 4123	16 977, 6491, 4461	32 272, 6250, 5448	4915, 1067, 1065
R_{int}	0.023	0.028	0.031	0.029	0.018
Refinement					
$R[F^2 > 2\sigma(F^2)]$, $wR(F^2)$, S	0.042, 0.114, 1.06	0.039, 0.117, 1.00	0.037, 0.111, 1.04	0.037, 0.098, 1.13	0.054, 0.133, 1.18
No. of reflections	3194	6520	6491	6250	1067
No. of parameters	244	447	445	408	75
No. of restraints	9	19	18	15	1
H-atom treatment	H atoms treated by a mixture of independent and constrained refinement	H atoms treated by a mixture of independent and constrained refinement	H atoms treated by a mixture of independent and constrained refinement	H-atom parameters constrained	H-atom parameters constrained
$\Delta\rho_{max}$, $\Delta\rho_{min}$ (e Å^{-3})	0.48, −0.37	0.41, −0.23	0.35, −0.28	0.44, −0.30	1.35, −1.10

Computer programs: *SMART* (Bruker, 2007*b*), *SAINT* (Bruker, 2007*a*), *SHELXTL*, *SHELXL*97 (Sheldrick, 2008).

2.2. Synthesis of $[Mn(acac)_2(H_2O)_2]NO_3 \cdot H_2O$

Manganese(II) acetate (1.00 g, 4.08 mmol) and acetylacetone (0.800 g, 8.29 mmol) were dissolved in 2.5 ml of water. To this solution solid ammonium ceric nitrate (3.30 g, 6.02 mmol) was added slowly while stirring. The green precipitate that formed was filtered off and dried. Different polymorphs were obtained by recrystallization of the precipitate as described below.

Polymorphs (1) and (2): The precipitate was dissolved in 3 ml of a 1:2 acetic acid–water mixture. In order to promote crystallization, 0.5 g of sodium nitrate was added to the above solution. The slight precipitate that formed upon dissolution of sodium nitrate was re-dissolved by adding a minimum amount of water. Green crystals formed within one day when the solution was kept at 273 K. While checking the crystals on the diffractometer, it was found that there were two types with similar block-type morphologies (prominent face with four or five edges) formed in nearly equal amounts. Yield: 0.370 g (1.00 mmol, 25%). Anal.: calc. for $MnC_{10}H_{20}NO_{10}$ (mol. wt 369.2): C 32.53, H 5.46, N 3.79; found: C 32.48, H 5.44, N 3.96. Important IR absorptions (KBr disk, cm^{-1}): 3441, 1969, 1753, 1628, 1537, 1426, 1350, 1277, 1030, 941, 810, 689, 633, 492 and 428.

Polymorphs (3) and (4): The precipitate was dissolved in 5 ml of water and 0.50 g sodium nitrate (0.50 g, 5.88 mmol) was added. The slight precipitate that formed was re-dissolved by adding a minimum amount of water. Crystals were formed within a few days when the solution was kept at 278 K. The majority of the crystals (about 60%) belonged to polymorph (1). About 40% of the crystals had a different morphology having prominent hexagonal faces. They belong to polymorph (3). Yet another polymorph, (4) (similar in shape to 1), was formed as a minor product. When crystallization was repeated several times, form (4) could only be isolated in two experiments. The total yield from crystallization from water was less than 5% due to decomposition of the Mn^{III} complex, as seen from the slow decolourization of the solution.

2.3. Synthesis $[Mn(acac)_2(H_2O)_2]BF_4 \cdot 2H_2O$ (5)

To a mixture of NH_4BF_4 (1.00 g, 9.54 mmol) and manganese(II) acetate in 5 ml water, acetylacetone (0.800 g, 8.29 mmol) was added. Powdered ammonium ceric sulfate was added slowly while stirring. A mixture of green and white precipitates was formed. The green precipitate was separated immediately by dissolving in a minimum amount of acetonitrile and drying on the water bath. Yield 0.576 g (1.36 mmol

Table 2
Metric parameters (Å, °) of the $[Mn(acac)_2(H_2O)_2]^+$ ion in various crystals.

Crystal	Ion (type)	$Mn-O_{equatorial}$	$Mn-O_{axial}$	δ†	Hydrogen bond $D\cdots A$ and $D-H\cdots A$
Polymorph (1)	Mn1 (I)	1.91, 1.91	2.23	3	2.72, 172; 2.90, 175
	Mn2 (II)	1.90, 1.90	2.20	29	2.68, 163; 2.70, 154
Polymorph (2)	Mn1 (II)	1.90, 1.91	2.21	22	2.75, 165; 2.75, 159
	Mn2 (II)	1.90, 1.91	2.21	21	2.75, 152; 2.75, 168
	Mn3 (I)	1.90, 1.91	2.23	2	2.91, 174; 2.72, 173
	Mn4 (I)	1.90, 1.91	2.23	3	2.89, 170; 2.74, 177
Polymorph (3)	Mn1 (I)	1.91, 1.91, 1.91, 1.91	2.23, 2.24	3, 3	2.90, 173; 2.74, 174 2.91, 173; 2.72, 172
	Mn2 (II)	1.91, 1.91	2.20	22	2.76, 155; 2.76, 163
	Mn3 (II)	1.91, 1.92	2.21	22	2.76, 164; 2.77, 157
Polymorph (4)	Mn1 (II)	1.90, 1.91, 1.91, 1.92	2.20, 2.20	25, 26	2.71, 160; 2.72, 157 2.71, 157; 2.74, 162
	Mn2 (I)	1.91, 1.91	2.22	1	2.86, 180; 2.71, 177
	Mn3 (I)	1.91, 1.92	2.23	5	2.84, 177; 2.75, 173
Compound (5)	Mn (I)	1.91, 1.91	2.23	12	2.64, 170; 2.75, 126

† Angle between the $Mn(O)_4$ mean plane and the plane of the three sp^2-C atoms of acac.

34%). Characteristic IR peaks (KBr disk cm^{-1}): 3462, 2484, 2363, 2320, 2137, 2054, 1977, 1543, 1523, 1340, 1032, 935, 694. C, H, N analysis: calc. for $C_{10}H_{22}MnO_8BF_4$ (mol. wt 412.04): C 29.15, H 5.38; found: C 30.09, H 5.12. X-ray quality crystals were obtained when this precipitate was dissolved in a minimum amount of a 1:1 acetic acid–water mixture and kept for crystallization at 273 K for several weeks.

2.4. X-ray crystallography

Data were collected on a Bruker SMART APEX CCD X-ray diffractometer using graphite-monochromated Mo $K\alpha$ radiation. The data were reduced using *SAINT-Plus* (Bruker, 2003), and multiscan absorption corrections were applied. The structures were solved using *SHELXS*97 and refined using *SHELXL*97 (Sheldrick, 2008). All ring H atoms were assigned on the basis of geometrical considerations and were allowed to ride upon the respective C atoms. All the water H atoms were located from the difference-Fourier maps and bond-length constraints were applied. In (1) the acetyl acetonate ligand in one of the two centrosymmetric cations was disordered over two positions. Every atom has 50% occupancy and was assigned directly from the Fourier peaks. In (5) BF_4^- was disordered over two inversion-related positions. Crystal data are reported in Table 1, while some important metric parameters are collected in Table 2. Powder diffraction patterns were calculated using *Mercury* software (Bruno *et al.*, 2002).

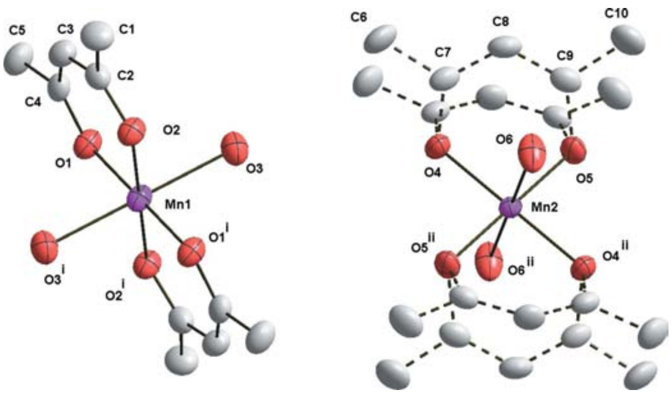

Figure 1
Displacement ellipsoid plot of the two crystallographically independent complex cations of polymorph (1). Here and in other displacement ellipsoid drawings, atoms are represented as 50% probability ellipsoids and ring as well as water H atoms have been omitted for clarity. Symmetry codes: (i) $-x, -y, -z$; (ii) $-x, -y, -z+1$.

2.5. Computational methods

Density-functional theory (DFT) calculations along with geometry optimization were carried out using the B3LYP exchange correlation functional (Becke, 1993) as implemented in *GAUSSIAN*03 (Frisch *et al.*, 2003). The spin-unrestricted version was employed for open-shell ions. For both types of calculations, triple-ζ basis sets (Schaefer *et al.*, 1994) were used for the Mn atom and double-ζ basis sets (Schaefer *et al.*, 1992) were used for all other atoms. Lattice energies of polymorphs (1), (2), (3) and (4) were computed using the crystal packer module in Version 4.8 of *Cerius*^{2} by energy minimization of crystal structures using Universal 1.02 force fields (Accelrys Inc., 2003). Electrostatic as well as van der Waals interactions were calculated by using the Ewald summation technique. Charges on atoms were calculated using the charge-equilibrium method. All of the calculations were carried out using the rigid-body method. Since all the structures have atoms on special positions, the calculations were carried out by converting the structures into crystalline superlattices.

3. Results and discussion

3.1. Synthesis and structure

The ability of $[Mn(acac)_2(H_2O)_2]^+$ to oxidize hypophosphite and HSO_3^- ions is known (Banerjee *et al.*, 1992; Gangopadhyay *et al.*, 1994; Mukhopadhyay & Banerjee, 1993). Unlike the Schiff bases and certain other ligands, acacH does not render aqueous Mn^{II} solutions susceptible to air oxidation. The previous preparation of the perchlorate salt of $[Mn(acac)_2(H_2O)_2]^+$ made use of MnO(OH) in glacial acetic acid as the starting material (Swarnabala *et al.*, 1994). In the present work, the nitrate salt was obtained as four polymorphs by Ce^{IV} oxidation in aqueous medium. The initial precipitate formed in this reaction is in all probability $[Mn^{III}(acac)_2(H_2O)_2]_3[Ce^{III}(NO_3)_6]$. This precipitate upon crystallization from methanol gave a good yield of crystals which analysed as $[Mn^{III}(acac)_2(CH_3OH)_2]_3$ $[Ce^{III}(NO_3)_6]$. The structure of this compound has been described elsewhere (Biju & Rajasekharan, 2010). However, aqueous solutions produced crystals only in the presence of excess nitrate, forming the four polymorphs.

The complex cation present in all the polymorphs is *trans*-$[Mn(acac)_2(H_2O)_2]^+$ (Figs. 1–4). One feature that is common to all the polymorphs is a Z' number greater than 1. Z' is defined here as the number of crystallographically different cations in the asymmetric unit. Taken together, there are 12 ions in all and all but two are located on crystallographic inversion centres. Only in one case is there a disorder owing to the positioning of the acac ligand. The metric parameters of the complex ion are collected in Table 2. In sharp contrast, the tetrafluoroborate salt (5) has only one complex ion in the asymmetric unit which is situated at the intersection of two crystallographic symmetry elements, *viz*. a twofold axis and a perpendicular mirror plane (Fig. 5).

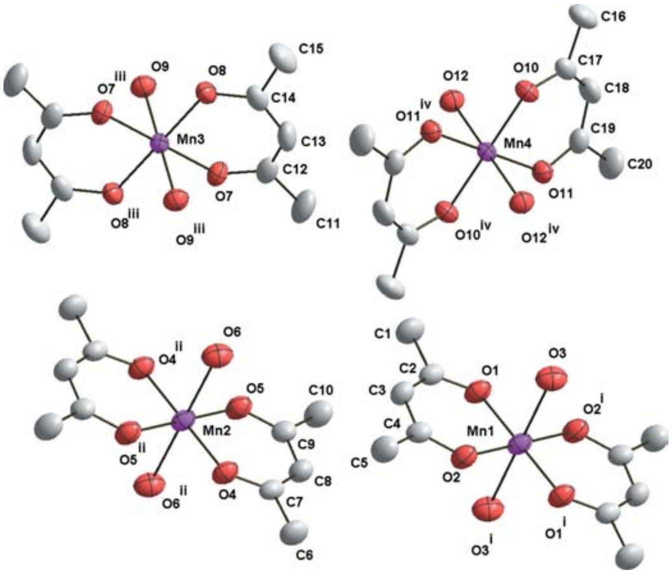

Figure 2
Displacement ellipsoid plot of the four crystallographically independent complex cations of polymorph (2). Symmetry codes: (i) $-x+1, -y, -z$; (ii) $-x, -y+1, -z$; (iii) $-x, -y+1, -z+1$; (iv) $-x+1, -y, -z+1$.

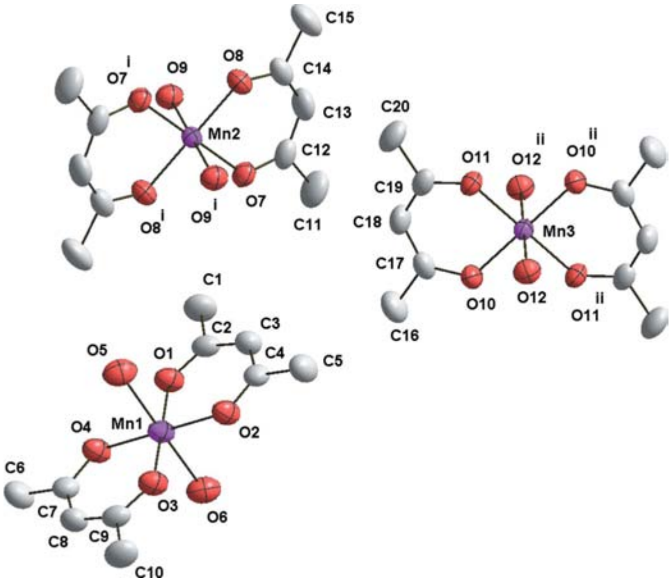

Figure 3
Displacement ellipsoid plot of the three crystallographically independent complex cations of polymorph (3). Symmetry codes: (i) $-x+1, -y+1, -z+1$; (ii) $-x, -y, -z+1$.

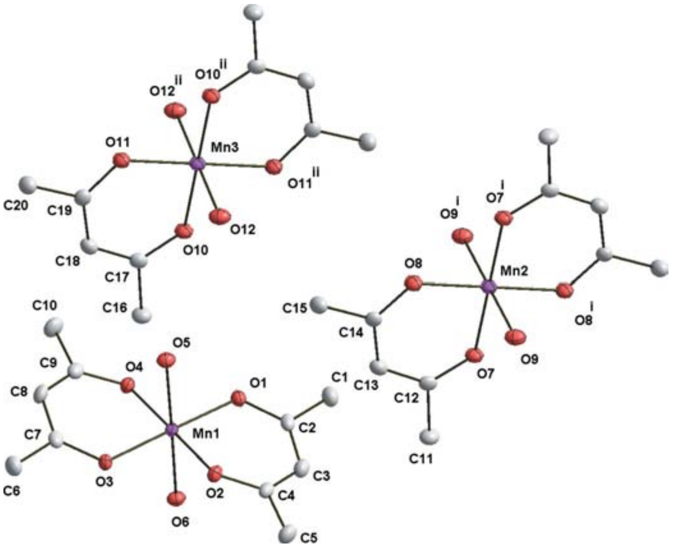

Figure 4
Displacement ellipsoid plot of the three crystallographically independent complex cations of polymorph (4). Symmetry codes: (i) $-x+1, -y+1, -z$; (ii) $-x, -y, -z$.

It is necessary to examine the four structures (1)–(4) to see whether they qualify to be termed polymorphs. This is required because, as recently pointed out by Bernstein *et al.* (2008), the technical advances in crystallography allow structure determination using more and more imperfectly grown crystal samples, often revealing a large number of molecules in the asymmetric unit. At the outset it may be seen from Table 1 that the crystals studied here do not suffer from gross imperfections [an $R_{\rm int}$ value of 0.03 with the ratio of measured to independent reflections greater than 2.5, about 65–85% of the independent reflections flagged as observed, and residuals (R) of only 0.04]. In order to probe further, the following studies were made:

(i) Simulation of the powder patterns: Fig. S10 of the supplementary material[1] shows the calculated powder patterns (Mo $K\alpha$, un-normalized) in the 2θ range 5–25°. As expected, the powder pattern of (4) is greatly different from those of the other three crystals. In order to make a closer comparison, Fig. 6 plots the patterns calculated for crystals (1)–(3) in the 2θ range 8–14°. It is seen that there are differences between the three patterns, which though not large, may still allow a distinction to be made between these three polymorphs based on their experimental powder patterns.

(ii) Mn—Mn distances have been calculated for all the crystallographically independent cations giving the following values (Å): polymorph (1), 7.80; polymorph (2), 7.71, 7.71, 7.98, 7.98, 10.95, 11.24; polymorph (3), 7.73, 8.01, 10.36; polymorph (4), 7.58, 7.96, 10.17. An overlap of points in the plot of

---

[1] Supplementary data for this paper are available from the IUCr electronic archives (Reference: ZB5009). Services for accessing these data are described at the back of the journal.

calculated intermolecular interaction energy *versus* intermolecular distance is an indication that the polymorphs are indistinguishable (Bernstein *et al.*, 2008). We have not calculated the intermolecular energies required for performing this test. Nevertheless, the fact that the number of intermolecular pairs is different for polymorphs (1)–(3) (different Z' values) indicates that these are independent polymorphs. Complementing this observation by the calculated powder patterns discussed above and the observed differences in the reduced unit cells, it seems appropriate to treat the four structures as polymorphic.

(iii) Pseudo-symmetry: As pointed out by a referee, there are certain pseudo-symmetric relationships between the independent molecules in structures (2), (3) and (4). In (2) the Mn3 cation is approximately related to the Mn4 cation by a C-centering operation, with a similar relationship being found between Mn1 and Mn2. Similarly, there is an approximate screw relationship between the Mn2 cation and the Mn3 cation. In both these structures, the overlays based on the relationships are good for all atoms except the O atoms of the axially coordinated water molecules. In polymorph (4) the Mn2 cation and the Mn3 cation are again related by a C-centring operation. In this case even the agreement of the axial water molecules is good, even though the two pseudo-symmetry related molecules differ slightly in the δ angle (Table 2). In all likelihood polymorphic diversity in the present system is related to the flexible coordination of the axial water molecules in the Jahn–Teller active cation and the flexibility of the chelate ring which is related to hydrogen bonding in the lattice.

Hydrogen bonding plays a very important role in the packing scheme of polymorphs (1)–(4) (Figs. S11–S15, supplementary material). All H atoms of the coordinated water molecules participate in hydrogen bonding. The complex ions can be classified into two types depending upon the hydrogen-bond acceptors involved. In the type I ion, one hydrogen from each coordinated water molecule is bonded to a nitrate oxygen, with the other bonded to a lattice water oxygen. The type II complex ion, on the other hand, has all the four H atoms bonded to nitrate O atoms. The resulting two-dimensional network, excluding the acac ions, is shown in Fig. 7. This network in which type II ions form one-dimensional chains which are then interconnected by the type I ions is present in all the polymorphs. There is an important difference between the two types of complex ions with regard to the geometry of the equatorial plane. For the type I ions, the plane of the acac C atoms is within 1–5° of the $Mn(O)_4$ coordination plane, while for type II ions there is a large distortion of 21–29°. The chelate in type II ions, therefore, has a chair conformation, while for type I it is nearly planar. Further, the axial Mn—O bond distances are in the range 2.23–2.24 Å for type I and 2.20–2.21 Å for type II. The above differences in coordination geometry, seen in all the polymorphs, appear to be imposed by the hydrogen-bonding interactions in the

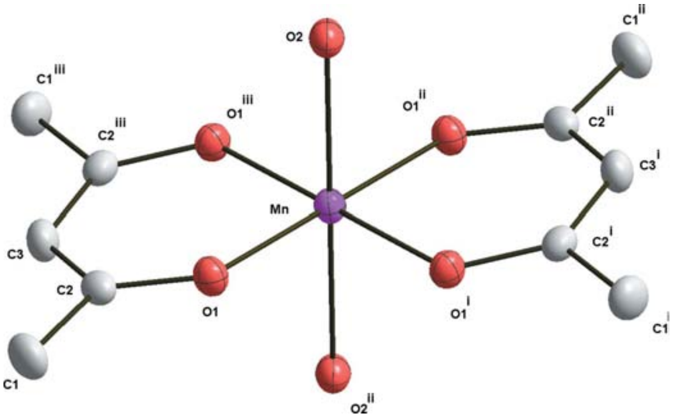

Figure 5
Displacement ellipsoid plot of the complex cation of (5). Symmetry codes: (i) $-x+1, y, -z$; (ii) $-x+1, -y, -z$; (iii) $x, -y, z$.

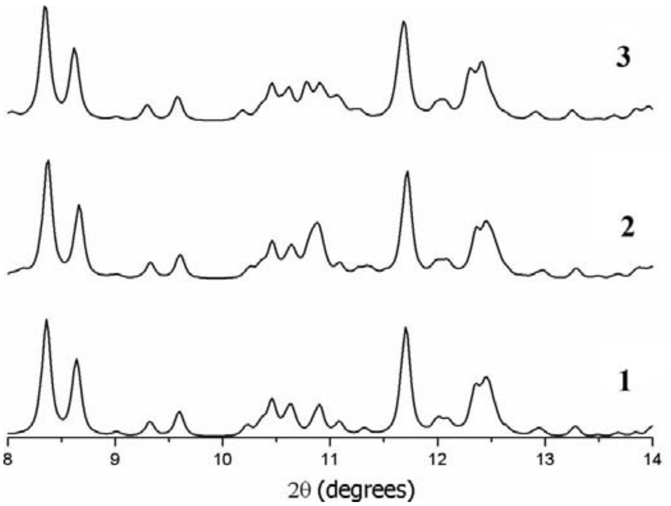

Figure 6
Calculated X-ray powder diffraction patterns for crystal structures (1)–(3).

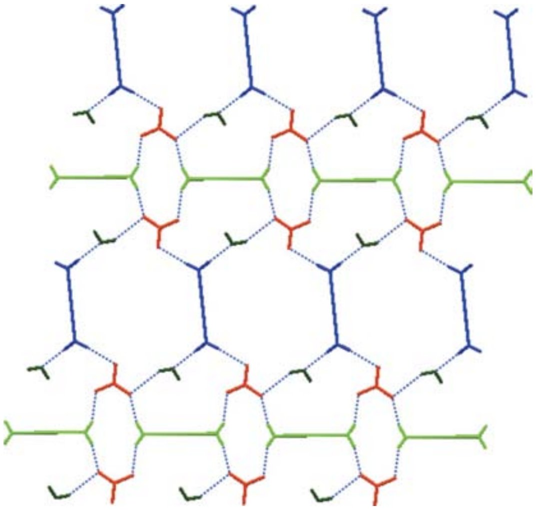

Figure 7
Two-dimensional network of hydrogen bonds seen in (1). The acac ligands have been omitted. In this and later figures blue and green denote type I and type II complex ions, respectively.

Table 3
Lattice energies ($U_{\rm latt}$, kJ mol^{-1}) of forms (1)–(4) (per molecule of [Mn(acac)$_2$(H$_2$O)$_2$]NO$_3$·H$_2$O).

$U_{\rm latt}$	(1)	(2)	(3)	(4)
Total	−616.05	−512.88	−506.56	−549.77
van der Waals	−108.15	−123.85	−117.02	−120.50
Coulombic	−507.90	−387.36	−389.54	−429.27

lattice. That intermolecular interactions can often extend a significant influence on coordination geometry has been previously noted (Swarnabala & Rajasekharan, 1996; Steed *et al.*, 2003). Important hydrogen-bond parameters are included in Table 2.

Even though the hydrogen-bonded water network shown in Fig. 7 is present in all the polymorphs, there are certain differences. Saturation with regard to hydrogen bonding is achieved by bonding the free hydrogen of the lattice water with the acac O atom. In terms of the details of this interaction, polymorph (1) is similar to (4), while polymorph (2) is similar to (3) (Fig. 8). However, as evident from Fig. 8, in terms of the overall packing, polymorph (4) is quite different from the other three. Lattices of (2) and (3) closely approach isomorphic as well as isostructural character, (1) has halved the translation along the *b* direction, while (4) forms a higher symmetry (monoclinic) lattice with the translation doubled along the *c* direction. Finally, in the tetrafluoroborate compound (5), [Mn(acac)$_2$(H$_2$O)$_2$]$^+$ ions form a two-dimensional hydrogen-bonded network with the help of lattice water molecules which are further organized into a three-dimensional structure by O—H···F interactions with the BF$_4$ anion (Figs. S16 and S17, supplementary material).

The hydrogen-bond patterns made up of 12-membered rings seen for the type II ions in the present polymorphs were also seen in various reported [ML(OH$_2$)$_2$](NO$_3$)$_2$ structures (CSD refcodes: AHAFEU, DUMBOC, DUMBUI, GIGZEB, HEXMIH, HEXMAZ, IRETUU, KAGMIP, LUFVIR and SUXPAC; CSD, Version 1.11, September 2009 release; Allen, 2002). The water–nitrate interaction in these structures interconnects the discrete units in one dimension. Some of the reported structures (CSD refcodes: DAPSCRIO, FELDAB, FODOEH, GAZTOQ, IWOZEB, TEMXIS, TEMXIS01, UGACOU and VIGDAQ) which contain [ML(OH$_2$)$_2$](NO$_3$)$_2$ as well as lattice water molecules do not show the above hydrogen-bond pattern. Instead, in all these structures lattice water molecules form hydrogen bonds with coordinated water molecules resulting in three-dimensional networks. One structure (CSD refcode: VEJNEE) that is stoichiometrically analogous to the present compound has a different hydrogen-bond pattern due to the ligand complexity. The above observations indicate that while one-dimensional chains of the 12-membered hydrogen-bond rings are widespread among anhydrous *trans*-[ML(OH$_2$)$_2$] dinitrates, the presence of lattice water generally disrupts this arrangement leading to three-dimensional motifs. The presence of lattice water in the present mononitrate coupled with ligand simplicity (with regard to hydrogen-bond donor/acceptor characteristics)

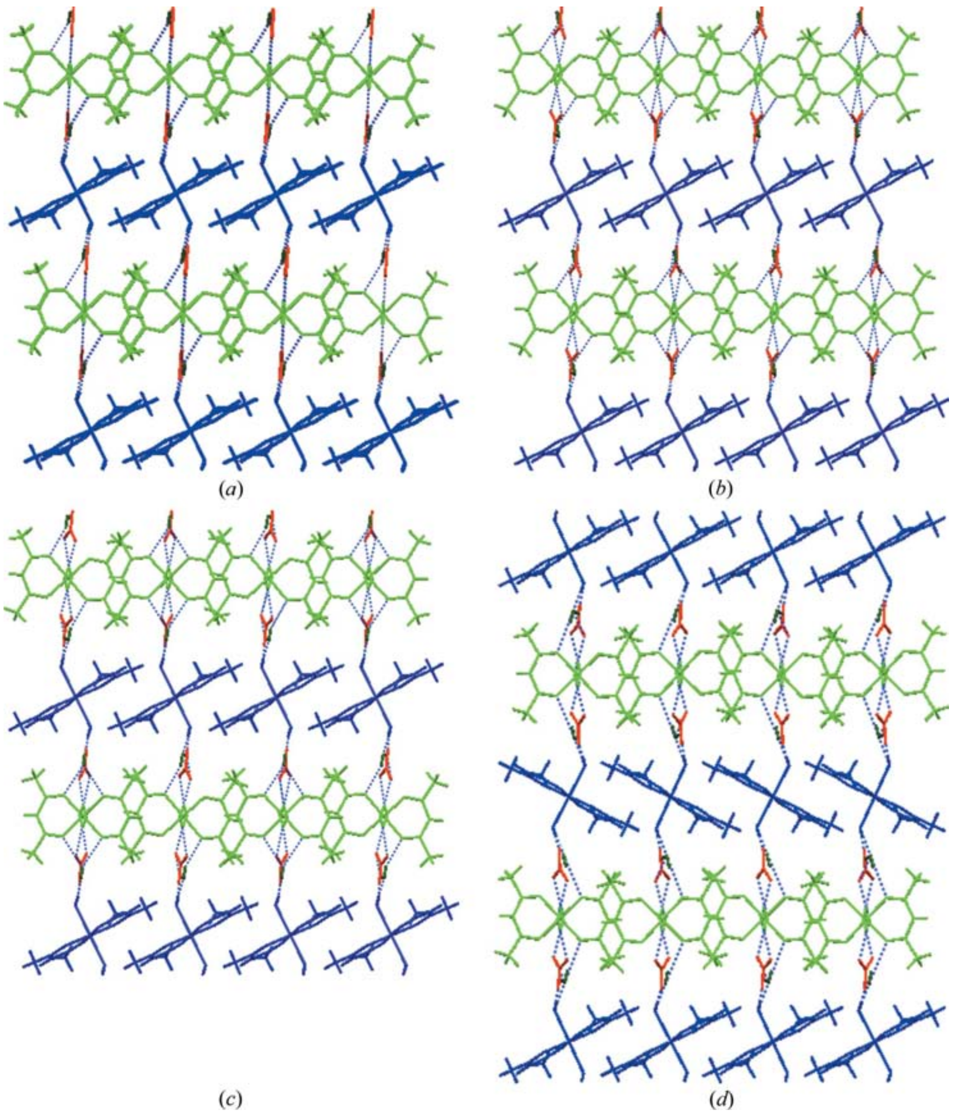

Figure 8
Crystal packing: (*a*) polymorph (1), viewed approximately down the [1 1 0] direction; (*b*), (*c*) and (*d*) represent polymorphs (2), (3) and (4), respectively, viewed down the *a* axis.

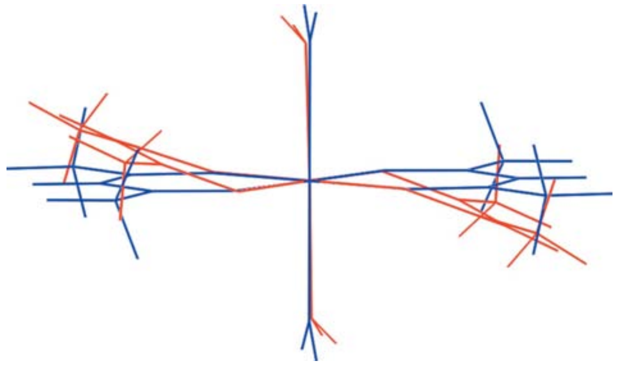

Figure 9
Optimized structure of the cation (planar chelate) superimposed on the crystallographic structure [Mn1 of structure (3), chair chelate].

leads to the incorporation of the 12-ring motif into a two-dimensional network.

3.2. Geometry optimization and lattice-energy calculations

The geometry optimization of the cationic part of (4) (Mn1) was carried out without any constraints. The optimized structure of the isolated cation is superimposed on a crystallographic structure (type II complex chosen for illustration) in Fig. 9. The bond distances in the optimized geometry are within 0.06 Å of the crystallographic values. Since the acetylacetonate group (excluding methyl H atoms) is coplanar with the Mn—O4 equatorial plane in the optimized structure, the deviation of it from the Mn—O4 plane for the actual molecules in the crystal may be considered as the criterion for stability. The structure with the smaller deviation will be more stable. So empirically, by counting the average deviation per molecule in the crystal, one can predict the stability of different forms of the polymorphs. The deviation (°) for each crystallographically distinct molecule in the crystal may be calculated by summing the δ values (Table 2) for the two halves of the bis-chelate. The average deviation, per molecule, for forms (1), (2), (3) and (4) is found to be 32.13, 24.72, 30.85 and 21.10, respectively. The order of stability is therefore (4) > (2) > (3) > (1). This order obviously does not take into account intermolecular interactions which are important for deciding the relative stabilities of the different polymorphs. The crystal lattice energies U_{latt} of polymorphs (1)–(4) were computed using *Cerius*^{2} (Table 3). The order of stability is now (1) > (4) > (2) > (3). As expected from the close similarity of the packing in (2) and (3) their lattice energies are equal within about 2%, while they are less stable than (4) and (1) by 8 and 25%, respectively. Form (1) is probably even more stable than found from the calculation because the entropic contribution arising from disorder is not included in the model. The decisive stability of form (1) over the others is reflected in its preferred crystallization from solution under different conditions.

4. Conclusion

Two types of complex ions, which are distortion isomers having different electronic stabilities, coexist in four different polymorphs having high Z'. All polymorphs are built around a two-dimensional extension, *via* lattice water molecules, of the previously known one-dimensional hydrogen-bond network involving two *trans*-coordinated water molecules and nitrate anions. Use of tetrafluoroborate (or perchlorate; Swarnabala *et al.*, 1994) did not lead to polymorphs under the conditions of preparation.

We thank the referees, whose comments have helped to improve the discussion on polymorphism and pseudo-symmetry. This work was supported by CSIR, India. ARB thanks UGC for a research fellowship. Infrastructure support from UGC (UPE program) and DST (X-ray diffractometer facility) is also acknowledged. DFT and *Cerius*^{2} calculations were performed using the CMSD facility, University of Hyderabad.

References

Accelrys Inc. (2003). *Cerius*^{2}, Version 4.8. Accelrys Inc., San Diego, USA, http://www.accelrys.com.
Allen, F. H. (2002). *Acta Cryst.* B**58**, 380–388.
Banerjee, R., Das, R. & Chakraburtty, A. K. (1992). *Transition Met. Chem.* **17**, 277–279.
Becke, A. D. (1993). *J. Chem. Phys.* **98**, 5648–5652.
Bernstein, J. (2002). *Polymorphism in Molecular Crystals.* Oxford University Press.
Bernstein, J., Dunitz, J. D. & Gavezzotti, A. (2008). *Cryst. Growth Des.* **8**, 2011–2018.
Biju, A. R. & Rajasekharan, M. V. (2010). *Cryst. Growth Des.* **10**, 426–429.
Bruker (2003). *SAINT-Plus.* Bruker AXS Inc., Madison, Wisconsin, USA.
Bruker (2007*a*). *SAINT*. Bruker AXS Inc., Madison, Wisconsin, USA.
Bruker (2007*b*). *SMART*. Bruker AXS Inc., Madison, Wisconsin, USA.
Bruno, I. J., Cole, J. C., Edgington, P. R., Kessler, M., Macrae, C. F., McCabe, P., Pearson, J. & Taylor, R. (2002). *Acta Cryst.* B**58**, 389–397.
Frisch, M. J. *et al.* (2003). *GAUSSIAN*03, Revision B.05. Gaussian, Inc., Pittsburgh, PA, USA.
Gangopadhyay, S., Ali, M. & Banerjee, P. (1994). *Coord. Chem. Rev.* **135/136**, 399–427.
Mukhopadhyay, S. & Banerjee, R. (1993). *J. Chem. Soc. Dalton Trans.* pp. 933–939.
Schaefer, A., Horn, H. & Ahlrichs, R. (1992). *J. Chem. Phys.* **97**, 2571-2577.
Schaefer, A., Huber, C. & Ahlrichs, R. (1994). *J. Chem. Phys.* **100**, 5829–5835.
Sheldrick, G. M. (2008). *Acta Cryst.* A**64**, 112–122.
Steed, J. W., Junk, P. C., Johnson, K. & Legido, C. (2003). *Polyhedron*, **22**, 769–774.
Swarnabala, G. & Rajasekharan, M. V. (1996). *Polyhedron*, **15**, 3197–3201.
Swarnabala, G., Reddy, K. R., Tirunagar, J. & Rajasekharan, M. V. (1994). *Transition Met. Chem.* **19**, 506–508.